



**UNIVERSIDADE DE SÃO PAULO**  
**FACULDADE DE CIÊNCIAS FARMACÊUTICAS DE RIBEIRÃO PRETO**

**Structural studies on *Trypanosoma cruzi* nitroreductase enzyme: characterization of prodrug activation mechanism for benznidazole and nifurtimox**

**Estudos estruturais da enzima nitrorredutase de *Trypanosoma cruzi*: caracterização do mecanismo de ativação dos pró-fármacos benznidazol e nifurtimox**

**MARÍLIA DE LIMA CIRQUEIRA**

Ribeirão Preto  
2019

**UNIVERSIDADE DE SÃO PAULO**  
FACULDADE DE CIÊNCIAS FARMACÊUTICAS DE RIBEIRÃO PRETO

**MARÍLIA DE LIMA CIRQUEIRA**

**Structural studies on *Trypanosoma cruzi* nitroreductase enzyme:  
characterization of prodrug activation mechanism for benznidazole and  
nifurtimox**

**Estudos estruturais da enzima nitrorredutase de *Trypanosoma cruzi*:  
caracterização do mecanismo de ativação dos pró-fármacos benznidazol e  
nifurtimox**

Master dissertation presented to the Graduate Program of School of Pharmaceutical Sciences of Ribeirão Preto/USP for the degree of Master in Sciences.

Concentration Area: Chemistry and Biological Physics

**Supervisor:** Prof. Dr. Maria Cristina Nonato

**Co-Supervisor:** Prof. Dr. Antônio José da Costa Filho

Corrected version of the Master's dissertation presented to the Graduate Program in Pharmaceutical Sciences on 02/08/2019. The original version is available at the School of Pharmaceutical Sciences of Ribeirão Preto.

Ribeirão Preto  
2019

I AUTHORIZE THE REPRODUCTION AND TOTAL OR PARTIAL DISCLOSURE OF THIS WORK, BY ANY CONVENTIONAL OR ELECTRONIC MEANS

Cirqueira, Marília de Lima

Structural studies on *Trypanosoma cruzi* nitroreductase enzyme: Characterization of prodrug activation mechanism for benznidazole and nifurtimox. Ribeirão Preto, 2019.

75 p.; 30 cm.

Master dissertation presented to the Graduate Program of School of Pharmaceutical Sciences of Ribeirão Preto/USP for the degree of Master in Sciences. Concentration Area: Chemical and Biological Physics

Supervisor: Nonato, Maria Cristina

Co-supervisor: Costa Filho, Antônio José

1. Nitroreductase 2. Chagas disease 3. *Trypanosoma cruzi* 4. Membrane protein

## APPROVAL PAGE

Marília de Lima Cirqueira

Structural studies on *Trypanosoma cruzi* nitroreductase enzyme: Characterization of prodrug activation mechanism for benznidazole and nifurtimox

Master dissertation presented to the Graduate Program of School of Pharmaceutical Sciences of Ribeirão Preto/USP for the degree of Master in Sciences.

Concentration Area: Chemistry and Biological Physics

**Supervisor:** Prof. Dr. Maria Cristina Nonato

**Co-Supervisor:** Prof. Dr. Antônio José da Costa Filho

Approved on:

Examiners

Prof. Dr. \_\_\_\_\_

Institution: \_\_\_\_\_ Signature: \_\_\_\_\_

## **Agradecimentos**

Gostaria de agradecer aos meus pais que me ensinaram que eu poderia fazer o que eu quisesse, mas que nada viria sem esforço. E além deles também aos meus irmãos, tios e tias, que cada um do seu jeito, me apoiaram e incentivaram nesse mestrado.

Ao meu namorado por me amparar nas inseguranças e sempre me incentivar.

À minha orientadora Cristina Nonato pela confiança em mim depositada, pelas correções que tanto me fizeram crescer e pelo apoio nas empreitadas.

Agradeço muito a todo time LCP-RP pelas discussões e teorias que me ajudaram na execução do meu projeto e companheirismo que tornou a caminhada mais agradável. Em especial a Iara e a Mariana pela amizade, paciência e pelas caronas.

Agradeço ao Professor Antônio José da Costa Filho pela disponibilização de equipamentos e materiais imprescindíveis para a conclusão deste trabalho e pelo auxílio na interpretação dos resultados.

Agradeço ao Professor Pietro Ciancaglini por disponibilizar o calorímetro de varredura diferencial e auxiliar nas interpretações dos resultados, juntamente com a Dra. Maytê Bolean.

Agradeço ao Professor Marcelo Dias Baruffi, pela disponibilização de equipamentos e materiais.

Gostaria de agradecer aos alunos do Laboratório de Biofísica Molecular, Laboratório de Nanobiotecnologia Aplicada: Sistemas Miméticos de Biomembranas e do Laboratório de Glicoimunologia que de uma forma ou de outra me ajudaram nas realizações dos experimentos e também pela companhia.

Agradeço à Professora Ana Paula Ramos por disponibilizar o tensiômetro OCA-20.

Agradeço à Professora Renata Viana Lopes por disponibilizar o equipamento Zetasizer.

Agradeço aos Professores João Santana e Ariel Silber pelo DNA genômico de *Trypanosoma cruzi* disponibilizado.

Agradeço ao Professor Shane Wilkinson por disponibilizar uma das construções gênicas utilizadas nesse trabalho.

O presente trabalho foi realizado com apoio da Coordenação de Aperfeiçoamento de Pessoal de Nível Superior – Brasil (CAPES) – Código de Financiamento 001.

“O correr da vida embrulha tudo, a vida é assim: esquenta e esfria, aperta e daí afrouxa, sossega e depois desinquieta. O que ela quer da gente é coragem.”

*João Guimarães Rosa*

## Resumo

Cirqueira, M. L. **Estudos estruturais da enzima nitrorredutase de *Trypanosoma cruzi*: Caracterização do mecanismo de ativação dos pró-fármacos benznidazol e nifurtimox.** 2019. 75f. Dissertação (Mestrado). Faculdade de Ciências Farmacêuticas de Ribeirão Preto – Universidade de São Paulo, Ribeirão Preto, 2019.

A doença de Chagas é uma antropozoonose causada pelo parasita *Trypanosoma cruzi* e que afeta aproximadamente 5 milhões de pessoas somente na América Latina, causando, no mundo todo, cerca de 10 mil mortes por ano. A doença de Chagas crônica tem grande impacto social e econômico devido a morbidade relacionada a mesma. O benznidazol é atualmente o único medicamento disponível no Brasil para o tratamento da doença de Chagas. Usado há mais de 40 anos, é caracterizado por baixa efetividade na fase crônica da doença, alta toxicidade e casos de resistência já foram relatados. Estudos demonstraram que os compostos nitroaromáticos, como o benznidazol, são pró-fármacos ativados pela redução do grupo nitro, gerando metabólitos citotóxicos, uma reação que é catalisada pela enzima nitrorredutase do tipo I (TcNTR), ausente no hospedeiro humano. Apesar de inúmeros esforços da comunidade científica, a estrutura tridimensional da TcNTR, assim como as bases moleculares e químicas de ativação seletiva dos pró-fármacos são ainda desconhecidas. Nesse contexto, esse trabalho teve objetivo iniciar os estudos de caracterização da enzima TcNTR, através do uso de uma gama de técnicas biofísicas e bioquímicas. Duas diferentes construções, TcNTR72 e TcNTR78, foram expressas, purificadas e foram avaliadas com relação a estabilidade química e térmica por meio de técnicas de fluorimetria de varredura diferencial (DSF) explorando o grupo prostético endógeno mononucleotídeo de flavina (FMN) como a sonda fluorescente (ThermoFMN), e por espalhamento dinâmico de Luz (DLS). Nossos estudos mostraram que a construção TcNTR72 é mais estável e a presença do detergente triton X-100 é fundamental para a manutenção da integridade estrutural da proteína. Técnicas de calorimetria de varredura diferencial (DSC) e de tensiometria foram cruciais para demonstrar pela primeira vez a interação da TcNTR com membranas modelo que mimetizam a membrana interna mitocondrial. Estudos de modelagem molecular baseado em homologia e por métodos *ab initio* sugerem que a enzima TcNTR se enovela de forma similar às NTRs de bactéria. Domínios estruturais preditos como essenciais para a dimerização assim como o sítio do FMN localizado na interface dimérica foram identificados como conservados. A maior diferença entre a enzima TcNTR e as proteínas homólogas em bactérias aparece pela inserção de um fragmento de 23 resíduos na TcNTR, predito enovelar na forma de hélice- $\alpha$ . Com base em nossos resultados e nas diferenças em termos de localização celular e função entre as enzimas TcNTR e de bactéria, nossos estudos sugerem que a região pode ser importante para a interação da TcNTR com a membrana interna na mitocôndria do parasita. A alta identidade sequencial compartilhada entre as enzimas de tripanossomatídeos sugerem que nossos achados poderão ser extrapolados para o estudo das NTRs de outros parasitas como *Leishmania spp* e *Trypanosoma brucei*.

Palavras chave: Nitrorredutase, doença de Chagas, *Trypanosoma cruzi*, proteína de membrana.

## Abstract

Cirqueira, M. L. **Structural studies on *Trypanosoma cruzi* nitroreductase enzyme: characterization of prodrug activation mechanism for benznidazole and nifurtimox.** 2019. 75f. Dissertation (Master). Faculdade de Ciências Farmacêuticas de Ribeirão Preto – Universidade de São Paulo, Ribeirão Preto, 2019.

Chagas disease is an anthroponosis caused by the parasite *Trypanosoma cruzi*, affecting approximately 5 million people in Latin America alone, and causing, worldwide, around 10 thousand deaths a year. Chronic Chagas disease have a major social and economic impact due to the disease causing disabilities. Benznidazole is currently the only drug available in Brazil for the treatment of Chagas disease. Used for more than 40 years, it is characterized by low effectiveness in the chronic phase, high toxicity and cases of resistance have been reported. Studies have shown that nitroaromatic compounds, such as benznidazole, are prodrugs activated by the reduction of the nitro group, generating cytotoxic metabolites, a reaction that is catalyzed by nitroreductase type I (TcNTR), absent in the human host. Despite several efforts by the scientific community, the three-dimensional structure of TcNTR, as well as the molecular and chemical bases of prodrugs selective activation are still unknown. In this context, this work aimed at initiating the characterization studies of the enzyme TcNTR, using a range of biophysical and biochemical techniques. Two different constructs, TcNTR72 and TcNTR78, were expressed, purified and evaluated for chemical and thermal stability by differential scanning fluorimetry (DSF), exploring the endogenous prosthetic group of flavin mononucleotide (FMN) as the fluorescent probe (ThermoFMN), and by dynamic light scattering (DLS). Our studies have shown that the TcNTR72 construct is more stable and the presence of the detergent Triton X-100 is critical for maintaining the structural integrity of the protein. Differential scanning calorimetry (DSC) and tensiometry techniques were crucial to demonstrate, for the first time, the interaction of TcNTR with model membranes that mimics the inner mitochondrial membrane. Homology and *ab initio* molecular modeling suggest that the folding of TcNTR is similar to bacterial NTRs. Structural domains predicted to be essential for dimerization as well as the site of FMN binding located at the dimeric interface were identified as conserved. The major difference between TcNTR enzyme and the homologous bacterial proteins appears to be the insertion of a 23 residues fragment in TcNTR, predicted to fold in the form of an  $\alpha$  helix. Based on our results and the differences in cell localization and function between TcNTR and bacterial enzymes, our studies suggest that the region may be important for the interaction of TcNTR with the parasite inner mitochondrial membrane. The high sequence shared among trypanosomatid NTRs enzymes suggests that our findings can be extrapolated to the study of NTRs from other parasites such as *Leishmania* spp. and *Trypanosoma brucei*.

Key words: Nitroreductase, Chagas disease, *Trypanosoma cruzi*, membrane protein.

## List of Figures

- Figure 1:** Schematic representation of the life cycle of *Trypanosoma cruzi*, etiologic agent of Chagas' disease: (1) infection of the triatomine by ingestion of trypomastigote forms; (2) metacyclic trypomastigote form; (3) differentiation in epimastigotes and spheromastigotes in the stomach; (4) binary division reproduction of the epimastigote forms in the intestine; (5) differentiation in metacyclic trypomastigotes in the rectum; (6) triatomine blood meal with elimination of the parasite by feces or urine; (7) metacyclic trypomastigotes enter the skin; (8) infection of macrophages with trypomastigotes; (9) lysosome containing the parasite; (10) differentiation into amastigotes; (11) multiplication of amastigotes in the cytoplasm; (12) differentiation into trypomastigotes; (13) rupture of the cell and release of trypomastigotes into the bloodstream; (14) amastigote and trypomastigote forms; (15) trypomastigotes (a) and amastigotes (b) infect new cells (Extracted from TEIXEIRA et al., 2012)..... 11
- Figure 2:** Current situation of Chagas disease in Latin America.(PÉREZ-MOLINA; MOLINA, 2017)..... 12
- Figure 3:** Chemical structure of the drugs benznidazole and nifurtimox. .... 13
- Figure 4:** Schematic representation of the full reduction of the nitrocompounds benznidazole and nifurtimox by nitroreductases (Extracted from PATTERSON; WYLLIE, 2014)..... 16
- Figure 5:** Representation of *T. cruzi* nitroreductase two substrate enzyme kinetics. .... 16
- Figure 6:** Cartoon representation of *E. coli* nitroreductase (PDB code: 1DS7) monomer (a) and dimer (b). .... 17
- Figure 7:** Scheme presenting a typical thermogram of a lipid phase transition and the effect of temperature in the acyl chains (Adapted from DEMETZOS, 2008).**Erro! Indicador não definido.**
- Figure 8:** Schematic representation of (a) basic pendand drop tensiometry experimental setup (BERRY et al., 2015) and (b) the basis of ADSA..... **Erro! Indicador não definido.**
- Figure 9:** Sequence alignment for nitroreductases from *Trypanosoma cruzi* (TcNTR), *Escherichia coli* (Ec), *Bacillus subtilis* (Bc), *Enterobacter clocae* (Ent), *Thermus thermophilus* NADH oxidase (TtNOX) and NAD(P)H:FMN oxidoreductase from *Vibrio fischeri* (FRase). Similarities in the sequence are highlighted in light gray. The residues were colored by their physicochemical properties: H, K, R – blue, polar and positively charged; D, E – red, polar and negatively charged; S, T, N, Q – green, polar and neutral; F, Y, W – pink, aromatics and non-polar; A, V, L, I, M – purple, aliphatic and non-polar; P, G - orange, small residues; C – yellow, not classified. The alignment was done using the server PROMALS3D (PEI et al., 2008).  
..... **Erro! Indicador não definido.**
- Figure 10:** Sequence alignment for nitroreductases from *Trypanosoma cruzi* (TcNTR), *Trypanosoma brucei* (TbNTR) and *Leishmania major* (LmNTR). Similarities in the sequence are highlighted in light gray. The residues were colored by their physicochemical properties: H, K, R – blue, polar and positively charged; D, E – red, polar and negatively charged; S, T, N, Q – green, polar and neutral; F, Y, W – pink, aromatics and non-polar; A, V, L, I, M – purple, aliphatic and non-polar; P, G – orange, small residues; C – yellow, not classified. The alignment was done using the server PROMALS3D (PEI et al., 2008)..... **Erro! Indicador não definido.**
- Figure 11:** Scheme representing the sequence of *Trypanosoma cruzi* nitroreductase type I (Genebank accession no. XP\_810645). Secondary structure predicted by JPred4 (Expasy, DROZDETSKIY et al., 2015). Highlighted in red is the putative mitochondrial targeting sequence, in yellow the residues that can be interacting with the prosthetic group FMN and

diamonds marks the starting residue of the constructs TcNTR72 and TcNTR78.....**Erro! Indicador não definido.**

**Figure 12:** Absorbance spectra of purified TcNTR78 exhibiting a two peaks spectra characteristic flavin profile. Maximum peak was found at 461 nm and used for protein quantification. .... **Erro! Indicador não definido.**

**Figure 13:** SDS-PAGE analysis of TcNTR78 purification showing the pure protein on lane 6 and 7 with the expected weight of around 30 KDa. .... **Erro! Indicador não definido.**

**Figure 14:** Consumption of NADH by TcNTR78 monitored by absorbance at 340 nm. ...**Erro! Indicador não definido.**

**Figure 15 :** Dynamic light scattering analysis of TcNTR78 solution showing its hydrodynamic diameter. .... **Erro! Indicador não definido.**

**Figure 16:** SDS-PAGE analysis for TcNTR78 expression. Soluble and insoluble fractions of cell culture for (a) different bacterial strains after induction at 17°C with two concentrations of IPTG and (b) the strain Rosetta™ after induction with different concentrations of IPTG with an induction at 25°C and 17°C..... **Erro! Indicador não definido.**

**Figure 17 :** SDS-PAGE analysis for TcNTR72 expression. Soluble (S, supernatant) and insoluble (P, pellet) fractions of cell culture showing the difference in autoinducted protein production with time and temperature using the bacterial strain Rosetta™.**Erro! Indicador não definido.**

**Figure 18:** SDS-PAGE analysis of TcNTR72 purification. The pure and tag free protein is showed in lane 7. .... **Erro! Indicador não definido.**

**Figure 19:** Consumption of NADH by TcNTR72 monitored by absorbance at 340 nm. ...**Erro! Indicador não definido.**

**Figure 20:** Absorbance spectra of construct TcNTR72 also exhibiting a maximum peak at 461 nm. .... **Erro! Indicador não definido.**

**Figure 21:** Size distribution of TcNTR72 solution obtained from DLS.**Erro! Indicador não definido.**

**Figure 22 :** Melting curves for both constructs monitored by the fluorescence of the FMN prosthetic group in presence of water. The sigmoidal fitting against the data was used to determine the melting temperatures found as 41 °C, 48 °C for TcNTR78 and TcNTR72, respectively..... **Erro! Indicador não definido.**

**Figure 23 :** Nitroreductase from *Escherichia coli* (PDB code: 1DS7) and *Thermus thermophilus* NADH oxidase (PDB code: 1NOX) in both cartoon and surface representation showing the solvent exposed flavin..... **Erro! Indicador não definido.**

**Figure 24 :** Comparison of the melting temperatures of constructs TcNTR78 and 72 by ThermoFMN..... **Erro! Indicador não definido.**

**Figure 25 :** Difference in Tm values of both constructs under different buffer conditions. The gray cells indicates no clear transition observed. A negative  $\Delta T_m$  higher than 2 °C is showed in red, in yellow the difference is lower than  $\pm 2^\circ\text{C}$  and in green the  $\Delta T_m$  is higher than 2°C. \* Multi-phasic unfolding. .... **Erro! Indicador não definido.**

**Figure 26:** Size distribution of TcNTR72 solution obtained from DLS Analysis of the different sodium chloride concentrations versus the size distribution. .... **Erro! Indicador não definido.**

**Figure 27 :** Influence of different sodium chloride concentrations on the melting temperature of the construct TcNTR72. .... **Erro! Indicador não definido.**

**Figure 28 :** Evaluation of the influence of sodium chloride concentration used in the purification buffer on TcNTR78 (a) and TcNTR72 (b) melting temperatures.**Erro! Indicador não definido.**

**Figure 29 :** Chemical structure of betaine and its non-detergent sulfonated derivatives: (1) betaine; (2) non detergent sulfobetaine 195/NDSB-195; (3) non-detergent sulfobetaine 201/NDSB-201; (4) non-detergent sulfobetaine 211/NDSB-211; (5) non-detergent sulfobetaine 221/NDSB-221; non detergent sulfobetaine 256/NDSB-256. ....**Erro! Indicador não definido.**

**Figure 30:** Analysis by ThermoFMN and DLS of the construct TcNTR72 purified with the addition of 10% of glycerol. No significant contribution was observed in terms of protein stability and homogeneity.....**Erro! Indicador não definido.**

**Figure 31:** SDS-page showing the purification of TcNTR72 without Triton X-100, in lane 6 we can observe the protein with the SUMO tag attached (approximately 42 kDa). Size distribution of the tag-free TcNTR72 after purification without the detergent.**Erro! Indicador não definido.**

**Figure 32:** DSC Thermogram. Effect of incubation time between DPPC liposomes and TcNTR on the lipid phase transition. Proportion of 1: 90000 in mols of protein: lipid was used.....**Erro! Indicador não definido.**

**Figure 33:** Effect of incubation on the thermal transition of DPPC liposomes with the construct TcNTR72 free of detergent (a) and filtered (b) in the proportion of 1: 90000 in mols of protein: lipid obtained by DSC. ....**Erro! Indicador não definido.**

**Figure 34:** Silver nitrate stained polyacrylamide gel electrophoresis (SDS-PAGE).....**Erro! Indicador não definido.**

**Figure 35:** Effect of incubation for 5 hours with SUMO tag protein on the phase transition peak of DPPC liposomes.....**Erro! Indicador não definido.**

**Figure 36:** DPPC liposomes thermograms and the effect of incubation with the TcNTR protein in different ratios and at different incubation times, as verified by DSC.**Erro! Indicador não definido.**

**Figure 37:** Thermograms obtained from liposomes of DPPC and DPPC: DPPE (3: 1) and the effect of incubation with the TcNTR protein, as verified by DSC.**Erro! Indicador não definido.**

**Figure 38:** Thermograms obtained from liposomes of DPPC: CL (3: 1) and DPPC: DPPE: CL (2: 1: 1) and the effect of incubation with the TcNTR protein, as verified by DSC. ....**Erro! Indicador não definido.**

**Figure 39:** Profile of the drop in the surface tension of the lipid monolayer constituted of DPPC (a) and DPPC:DPPE:CL (2:1:1) molar ratio (b) after the insertion of the TcNTR, verified by the axissimetric analysis of the drop form.....**Erro! Indicador não definido.**

**Figure 40:** Emission spectra of the fluorescence for TcNTR72 and the influence of DPPC liposomes.....**Erro! Indicador não definido.**

**Figure 41:** Differential scanning calorimetry of the construct TcNTR72 with and without the detergent Triton X-100. The large exothermic peak at 60°C corresponds to the detergent phase transition. ....**Erro! Indicador não definido.**

**Figure 42:** Thermograms (calorific capacity versus temperature) of TcNTR72 without detergent at 0.25, 0.5 and 0.95 mg/mL. ....**Erro! Indicador não definido.**

**Figure 43:** Cartoon representation of *Thermus thermophilus* NADH oxidase (a) and TcNTR models (b, homology-based; c, ab initio). ....**Erro! Indicador não definido.**

**Figure 44:** Cartoon representation in stereo view of TcNTR structure models. Superposition between the homology based (pink) and ab initio model (cyan) for TcNTR. **Erro! Indicador não definido.**

**Figure 45:** Cartoon representation of TcNTR model built in the server Swiss-Model as a monomer (a) and dimer (b). This model enabled the insertion of the prosthetic group FMN (c) since the putative binding site composed of the residues R88, S90, K92, Q145, E260 and R300 is conserved (d)..... **Erro! Indicador não definido.**

## List of Tables

**Table 1:** Protein solution conditions tested for crystallization in sparse matrix commercial kits and optimization attempts..... **Erro! Indicador não definido.**

**Table 2:** Additives with a positive shift above 3°C in at least one construct. Reference values: TcNTR72 – Tm = 47.20 °C/slope = 7.1 ΔI/K; TcNTR78 – Tm = 44.36°C/slope = 6.6 ΔI/K. .... **Erro! Indicador não definido.**

**Table 3:** Detergents that presented a positive influence in the protein thermal stability, both constructs in comparison. Reference values: TcNTR72 - Tm = 44.0°C/slope = 7.0 ΔI/K; TcNTR78 – Tm = 41.32°C/slope = 6.0 ΔI/K. Differences between both constructs as well as some degree of lack of reproducibility was observed and could be explained as a results of differences in the final Triton X-100 concentration for each batch of purification. .... **Erro! Indicador não definido.**

**Table 4:** Thermodynamic parameters obtained by DSC and size evaluation of liposome samples by DLS for DPPC liposomes and the effect of the different incubation time with TcNTR. .... **Erro! Indicador não definido.**

**Table 5:** Thermodynamic parameters obtained by DSC and size evaluation of liposome samples by DLS for DPPC liposomes and the effect of incubation for 5 hours with TcNTR protein after removal of Triton X-100 detergent and after removal of the aggregates by filtering with 0.8 μm filter. .... **Erro! Indicador não definido.**

**Table 6:** Thermodynamic parameters obtained by DSC and size evaluation of liposome samples by DLS for DPPC liposomes and the effect of incubation with SUMO tag protein. .... **Erro! Indicador não definido.**

**Table 7:** Thermodynamic parameters obtained by DSC and size evaluation of liposome samples by DLS for DPPC liposomes and the effect of TcNTR in different proportions and incubation time. .... **Erro! Indicador não definido.**

**Table 8:** Thermodynamic parameters obtained by DSC and size evaluation of liposome samples by DLS for DPPC and DPPC: DPPE (3: 1) liposomes and the effect of incubation with TcNTR. .... **Erro! Indicador não definido.**

**Table 9:** Thermodynamic parameters obtained by DSC and size evaluation of liposome samples by DLS for liposomes of DPPC:CL (3:1) and DPPC: DPPE:CL (2:1:1) and the effect of incubation with TcNTR. \* peak 1; \*\* peak 2. .... **Erro! Indicador não definido.**

## List of Abbreviations

<b>CL</b>	Cardiolipin - 1,3-bis(sn-3'-phosphatidyl)-sn-glycerol
<b>Cp</b>	Calorific capacity
<b>DLS</b>	Dynamic light scattering
<b>DPPC</b>	1,2-dipalmitoyl-sn-glycero-3-phosphocholine
<b>DPPE</b>	1,2-Dimyristoyl-sn-glycero-3-phosphocholine
<b>DSC</b>	Differential scanning calorimetry
<b>DSF</b>	Differential scanning fluorimetry
<b>DTT</b>	Dithiothreitol
<b>FMN</b>	Flavin mononucleotide
<b>IPTG</b>	Isopropyl $\beta$ -D-1-thiogalactopyranoside
<b>kDa</b>	KiloDalton
<b>LB</b>	Lysogeny broth
<b>NADH</b>	Nicotinamide adenine dinucleotide
<b>NTR</b>	Nitroreductase
<b>PDB</b>	Protein Data Bank
<b>PMSF</b>	Phenylmethylsulfonyl fluoride
<b>SUMO</b>	Small Ubiquitin Modifier
<b>Tb</b>	<i>Trypanosoma brucei</i>
<b>Tc</b>	<i>Trypanosoma cruzi</i>
<b>Tm</b>	Melting temperature
<b>ULP1</b>	Ubiquitin like protease 1

## Sumário

<b>Resumo</b> .....	i
<b>Abstract</b> .....	ii
<b>List of Figures</b> .....	iii
<b>List of Tables</b> .....	vi
<b>1. Introduction</b> .....	9
1.1. Chagas Disease .....	9
1.2. Nitroreductases (NTRs) .....	14
<b>2. Objectives</b> .....	<b>Erro! Indicador não definido.</b>
<b>3. Materials and methods</b> .....	<b>Erro! Indicador não definido.</b>
3.1. Cloning .....	<b>Erro! Indicador não definido.</b>
3.2. Expression .....	<b>Erro! Indicador não definido.</b>
3.3. Purification .....	<b>Erro! Indicador não definido.</b>
3.4. Determination of protein extinction coefficient based on prosthetic group FMN. ....	<b>Erro! Indicador não definido.</b>
3.5. Activity test .....	<b>Erro! Indicador não definido.</b>
3.6. Evaluation of protein thermal stability .....	<b>Erro! Indicador não definido.</b>
3.7. Evaluation of protein solution dispersity .....	<b>Erro! Indicador não definido.</b>
3.8. Evaluation of salt concentration on protein stability .....	<b>Erro! Indicador não definido.</b>
3.9. Evaluation of Triton X-100 on protein stability .....	<b>Erro! Indicador não definido.</b>
3.10. Crystallization experiments .....	<b>Erro! Indicador não definido.</b>
3.11. Protein-membrane interaction .....	<b>Erro! Indicador não definido.</b>
3.11.1. Differential Scanning Calorimetry .....	<b>Erro! Indicador não definido.</b>
3.11.2. Pendant drop tensiometry .....	<b>Erro! Indicador não definido.</b>
3.11.3 Fluorescence spectroscopy .....	<b>Erro! Indicador não definido.</b>
<b>4. Results</b> .....	<b>Erro! Indicador não definido.</b>
4.1. Expression and purification optimization .....	<b>Erro! Indicador não definido.</b>
4.2. Analysis of membrane interaction .....	<b>Erro! Indicador não definido.</b>
4.3. DSC analysis of TcNTR72 .....	<b>Erro! Indicador não definido.</b>
4.4. Crystallization experiments .....	<b>Erro! Indicador não definido.</b>
4.5. Structure models .....	<b>Erro! Indicador não definido.</b>
<b>5. Final remarks and future perspectives</b> .....	18
<b>Bibliography</b> .....	19

## 1. Introduction

### 1.1.Chagas Disease

Chagas disease or American trypanosomiasis is an antropozoonosis caused by the protozoan *Trypanosoma cruzi*, found naturally only in the American continent. Initially, it was believed that the *T. cruzi* clade evolved after the separation of South America and Africa. However, recent evidences indicate that *T. cruzi* evolved from a particular genotype found mostly in bats called TcBat and switched to terrestrial mammals through invertebrate vectors. *T. cruzi* has an extensive wild reservoir, especially mammals such as anteaters, armadillos, small primates and bats but there is no evidence of a negative impact in these natural hosts (GUHL; AUDERHEIDE; RAMÍREZ, 2014).

Chagas disease is pre-historical. Evidences suggests that human infections with *T. cruzi* occurred as soon as the South America was populated. The DNA of *T. cruzi* and classical signs of Chagas disease was found in a preserved mummy from 9000 years ago, where today is the south of Peru and the north of Chile. This finding generated the hypothesis that humans could have become hosts after the ingestion of the insect vector (triatomines) itself or the raw meat of infected animals. After the acquisition of sedentary habits and the domestication of animals, the triatomine vectors were attracted to live in the dwellings, made of mud and wood, initiating the domestic cycle of *T. cruzi* (ARAÚJO et al., 2009; STEVERDING, 2014).

Description of Chagas disease symptoms were found in records from travelers and physicians after the colonization of the American continent. However only in 1909 the Brazilian physician Carlos Chagas, in an expedition to the north of Minas Gerais state of Brazil, discovered the protozoan and named after his advisor, Oswaldo Cruz, as *Trypanosoma cruzi*. The flagellate was observed inside the hematophagous kissing bugs, abundant in that region, in the blood of domestic and wild animals, as well as, in infected patients with characteristic acute phase symptoms. Carlos Chagas described the transmission cycle, the vector, the etiological agent and the acute and chronic phase symptoms of the disease (COURA, 1997; KROPF, 2006; STEVERDING, 2014).

Chagas disease is endemic in Latin America where around 5 million people are infected, being a major public health problem (WHO, 2015). Only in Brazil, more than 1 thousand cases of acute Chagas disease were reported between 2012 and 2016. However,

the real number can be substantially higher and underreported must be considered since the disease is not always identified in its acute phase (BRASIL, 2019).

Worldwide, around 10 thousand deaths a year is caused by Chagas disease (WHO, 2010). The economic burden is estimated in US\$ 7.2 billion in health care costs and US\$1.2 billion loss in productivity due to associated morbidity and mortality (LEE et al., 2013; STANAWAY; ROTH, 2015). The majority (90%) of the burden affects endemic countries and the major risk of infection is among underprivileged population with poor housing quality (LEE et al., 2013). The World Health Organization considers Chagas disease a neglected illness due to the lack of proportional investments to the the number of infected people, along with other parasitic diseases that affect mostly developing countries (WHO, 2010).

The life cycle of *Trypanosoma cruzi* involves distinct forms both in the insect vector and in the vertebrate host (Figure 1). The vectorial transmission occurs through cutaneous penetration of the metacyclic trypomastigote form, released in the feces of its vector, the triatomine insect, after its blood meal. Entering the bloodstream, the trypanosomatid is internalized by cells such as macrophages, muscle or nerve cells, developing intracellularly in their amastigote form and subsequently differentiating into trypomastigotes. These, after cell disruption, are released into the extracellular space, infecting new cells or infecting another triatomine during their blood meal (TEIXEIRA et al., 2012). During a process known as metacyclogenesis, bloodstream trypomastigotes differentiate into the replicative form named epimastigote in the host insect's stomach. After migrating to the insect's rectum, the epimastigotes differentiate into the non-replicative, infective metacyclic trypomastigote, completing the life cycle (GONÇALVES et al., 2018) (Figure 1).

After the discovery of the transmission cycle, several programs to control the disease insect vector were successfully implemented. Improvement of housing quality and application of insecticides led to the interruption of the transmission by the triatomine in most areas of Brazil (Figure 2). However, about 13% of Latin American population is still at risk of *T. cruzi* infection due to poor house conditions or active transmission (WHO, 2015).

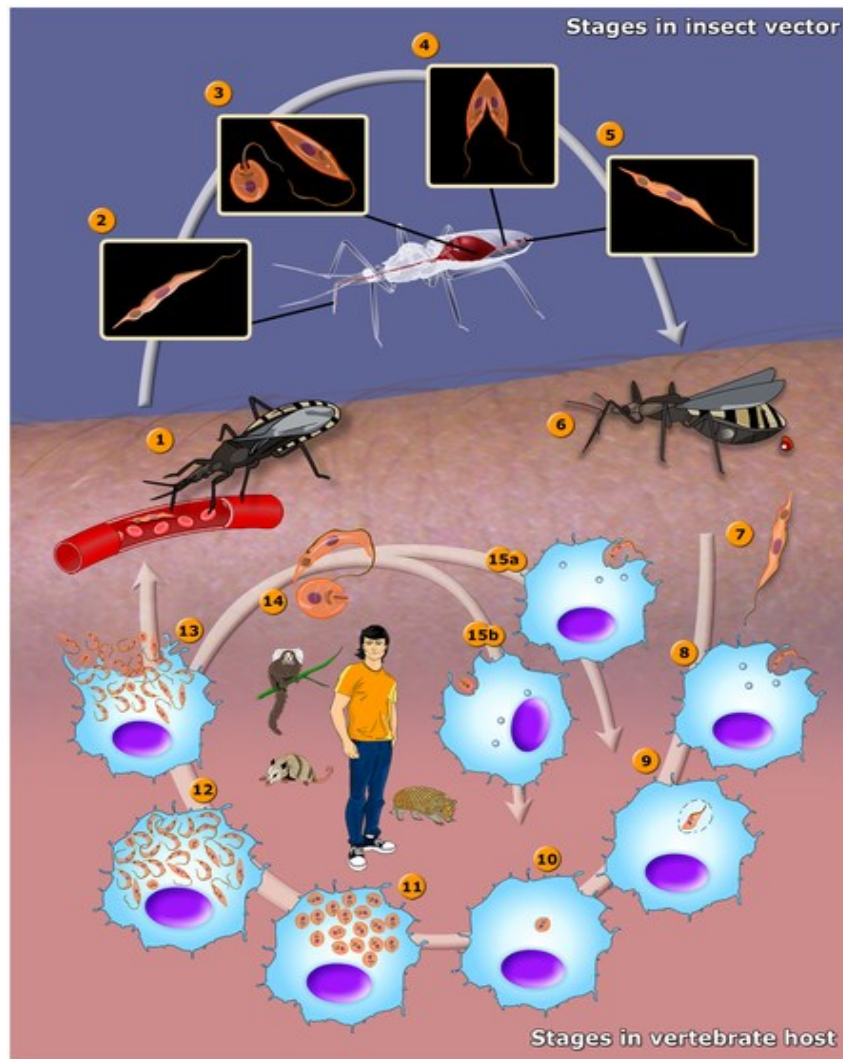


**Figure 1:** Schematic representation of the life cycle of *Trypanosoma cruzi*, etiologic agent of Chagas' disease: (1) infection of the triatomine by ingestion of trypomastigote forms; (2) metacyclic trypomastigote form; (3) differentiation in epimastigotes and spheromastigotes in the stomach; (4) binary division reproduction of the epimastigote forms in the intestine; (5) differentiation in metacyclic trypomastigotes in the rectum; (6) triatomine blood meal with elimination of the parasite by feces or urine; (7) metacyclic trypomastigotes enter the skin; (8) infection of macrophages with trypomastigotes; (9) lysosome containing the parasite; (10) differentiation into amastigotes; (11) multiplication of amastigotes in the cytoplasm; (12) differentiation into trypomastigotes; (13) rupture of the cell and release of trypomastigotes into the bloodstream; (14) amastigote and trypomastigote forms; (15) trypomastigotes (a) and amastigotes (b) infect new cells (Extracted from TEIXEIRA et al., 2012).

Nowadays, other forms of transmission, such as congenital, blood transfusion and organ transplantation, contributes to the spread of Chagas disease outside the endemic areas especially among migrant population (CONNERS et al., 2016; PÉREZ-MOLINA et al., 2015; ROBERTSON et al., 2016). This fact demanded the implementation of blood donor screening for *T. cruzi* DNA in the United States in 2007 (MARTIN et al., 2014).

Oral transmission, due to the ingestion of food contaminated with excrements or crushed parts of triatomines, has gained increased attention, and become a major issue in Brazil. It is found that 73% of Chagas disease acute cases reported between 2012 and 2016 were due to this type of transmission in Brazil (BRASIL, 2019).

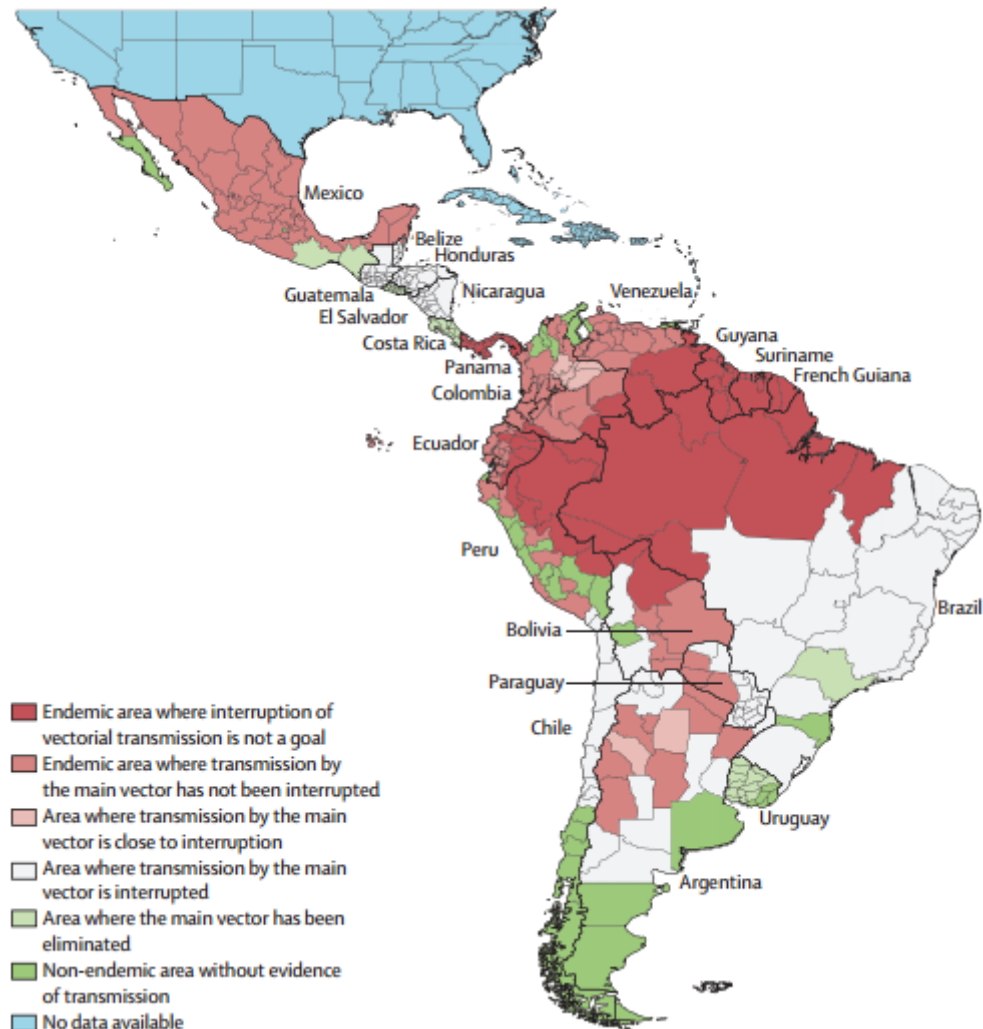


**Figure 2:** Current situation of Chagas disease in Latin America.(PÉREZ-MOLINA; MOLINA, 2017).

The clinical course of Chagas disease, composed by three phases, is highly related to genetic factors of the parasite and the host. The first phase, named acute, lasts around 2 to 4 weeks and presents unspecific symptoms, similar to those of other illnesses, such as fever and malaise. Despite being characterized by an abundant parasitemia that can be seen relatively easily by direct blood examination, the acute stage, in the majority of cases, is solved spontaneously, making its diagnosis very difficult. In only 2 to 3% of the cases, the acute phase can be life threatening due to acute myocarditis. The symptomatic acute phase is followed by an asymptomatic period of variable length that can last 10

years to life long and is characterized by non-detectable blood parasitemia. Reactivation of the acute phase can be observed due to host compromised immune response related to other comorbidities such as cancer and HIV infection (PEREZ; LYMBERY; THOMPSON, 2015). The last phase, named chronic, occurs in around 40% of infected people, characterized by cardiomyopathy and/or megagastrointestinal syndromes (PÉREZ-MOLINA; MOLINA, 2017).

A treatment for Chagas disease was made available only 50 years after the discovery of its causative agent. In 1966 benznidazole was released by Roche and later, in 1970, Bayer launched nifurtimox, which correspond to the only available drugs hitherto (Figure 3) (STEVERDING, 2014). Both compounds, however, cause harmful side effects ranging from cutaneous rash to blood marrow depletion. They have limited effectiveness in the chronic phase and resistant strains are reported. In Brazil only benznidazole is approved due to the higher toxicity displayed by nifurtimox (PÉREZ-MOLINA; MOLINA, 2017). Currently, an international multicentric trial called the BENEFIT project is evaluating the relevance of benznidazole treatment in late stage Chagas disease especially in patients with cardiovascular complications (MARIN-NETO et al., 2009). And nifurtimox, in combination with eflornithine is the recommended therapy for late stage African trypanosomiasis (HALL; BOT; WILKINSON, 2011a).

Benznidazole is a 2-nitroimidazole and nifurtimox a 5-nitrofurans. Thus, the chemotherapeutic potential of nitroheterocyclics compounds, especially for trypanosomatid related diseases cannot be underestimated and should be exploited. These are considered prodrugs, being activated by the reduction of their nitro groups and formation of cytotoxic metabolites. This reaction occurs inside the parasites by an enzyme called nitroreductase (NTR) (WILKINSON et al., 2008).

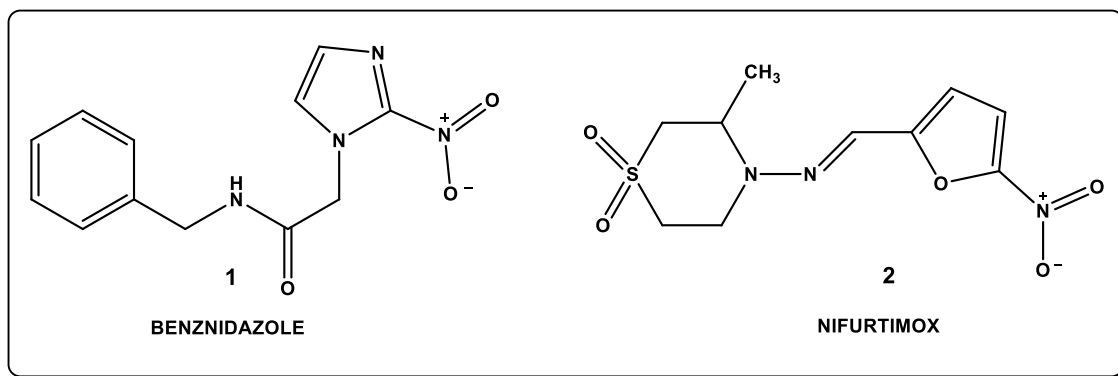


**Figure 3:** Chemical structure of the drugs benznidazole and nifurtimox.

## 1.2. Nitroreductases (NTRs)

NTRs are flavin dependent enzymes being classified into two categories, a type I, oxygen insensitive, promotes a sequential two-electron reduction in nitro groups to produce amine via hydroxylamine and nitroso derivatives, and type II, oxygen sensitive catalyze a one-electron reduction into a nitro anion radical which can be reoxidized in the presence of oxygen to the nitro group, producing superoxide anions as a result of the futile cycle. Type I nitroreductases can be further divided into two groups, a group A nitroreductases are usually NADPH-dependent and share higher similarity with NfsA (oxygen-insensitive NADPH nitroreductase that reduces nitrofurazone) from *Escherichia coli*, and group B nitroreductases may use both NADH and NADPH as electron donors and are represented by *E. coli* NfsB (oxygen-insensitive NAD(P)H nitroreductase that reduces a variety of nitroaromatic compounds including nitrofurazone, quinones, nitroimidazoles, among others) (PATTERSON; WYLLIE, 2014; ROLDÁN et al., 2008).

Type I NTRs are mainly found in bacteria and some fungus species although protozoans such as *Trypanosoma* sp. and *Leishmania* sp. are exceptions believed to acquire this enzyme by lateral gene transfer (DE OLIVEIRA; HENRIQUES; BONATTO, 2007). The *T. cruzi* enzyme (TcNTR) is a type I nitroreductase that have a flavin mononucleotide (FMN) as prosthetic group, uses nicotinamide adenine dinucleotide (NADH) as a cofactor and is found in the large single mitochondrion of the parasite (WILKINSON et al., 2008a).

It has been observed that the induced loss of NTR genes in *T. cruzi* not only induced a higher resistance to benznidazole, nifurtimox and other nitro compounds but also decreased the growth rate of the parasites in its epimastigote form and prevented the differentiation into the infective form (metacyclic trypomastigotes), indicating an important metabolic role of TcNTR in the parasite. Also, the enzyme could not be deleted from blood stream forms of *Trypanosoma brucei* where the NTR could be essential for this stage form (WILKINSON et al., 2008a). The loss of NTR gene and its downregulation is also observed in *Trypanosoma cruzi* with induced resistance to benznidazole (MEJÍA-JARAMILLO et al., 2011). Nonsense and missense mutations have also been identified in drug-resistant parasites, although diverse mechanisms are involved in the resistance (CAMPOS et al., 2014; MEJIA et al., 2012).

A *T. cruzi* prostaglandin F<sub>2</sub> $\alpha$  synthase or old yellow enzyme (OYE) is a NAD(P)H flavin oxidoreductase that also mediates a type I reduction of nitrocompounds but only under anaerobic conditions *in vitro*. This enzyme has no homolog in *T. brucei* and is suggested that it participates in benznidazole activation along with TcNTR. TcOYE is overexpressed when resistant parasites loses the NTR gene, and, under persistent drug exposure, the TcOYE gene is inactivated, being also involved in the mechanism of resistance (GARCÍA-HUERTAS et al., 2017; MURAKAMI et al., 2013). This way, NTR is believed to be the main activator of nitrocompounds used as prodrugs for Chagas disease.

For benznidazole, TcNTR and TbNTR promotes a serial 2 electron reduction in the drugs nitro group resulting in formation of nitrenium, dihydro-dihydroxy imidazole and glyoxal which reacts with thiols, proteins and nucleic acids causing cell damage (Figure 4). The redox reaction of the substrate follows a bi-bi ping pong mechanism of kinetics where initially the NADH is oxidized by the concomitant reduction of FMN. The nitrocompound is then reduced by FMNH<sub>2</sub>, thereby regenerating oxidized flavin competent for further catalytic cycles (Figure 5) (HALL; WILKINSON, 2012; PATTERSON; WYLLIE, 2014).

In nifurtimox metabolism, unlike benznidazole, it is demonstrated the generation of superoxide anions. Until this moment, only NTR was confirmed to activate the drug but does not follow a classic ping pong kinetics, possibly due to more than one mechanism of activation. Nifurtimox also produces a hydroxylamine through a nitroso intermediate which can be further metabolized to a nitrenium ion or an open chain nitrile, which is highly toxic (even to mammalian cells) possibly due to non-specific reaction with a range of cellular molecules as it can function as a Michael acceptor (HALL; BOT; WILKINSON, 2011b).

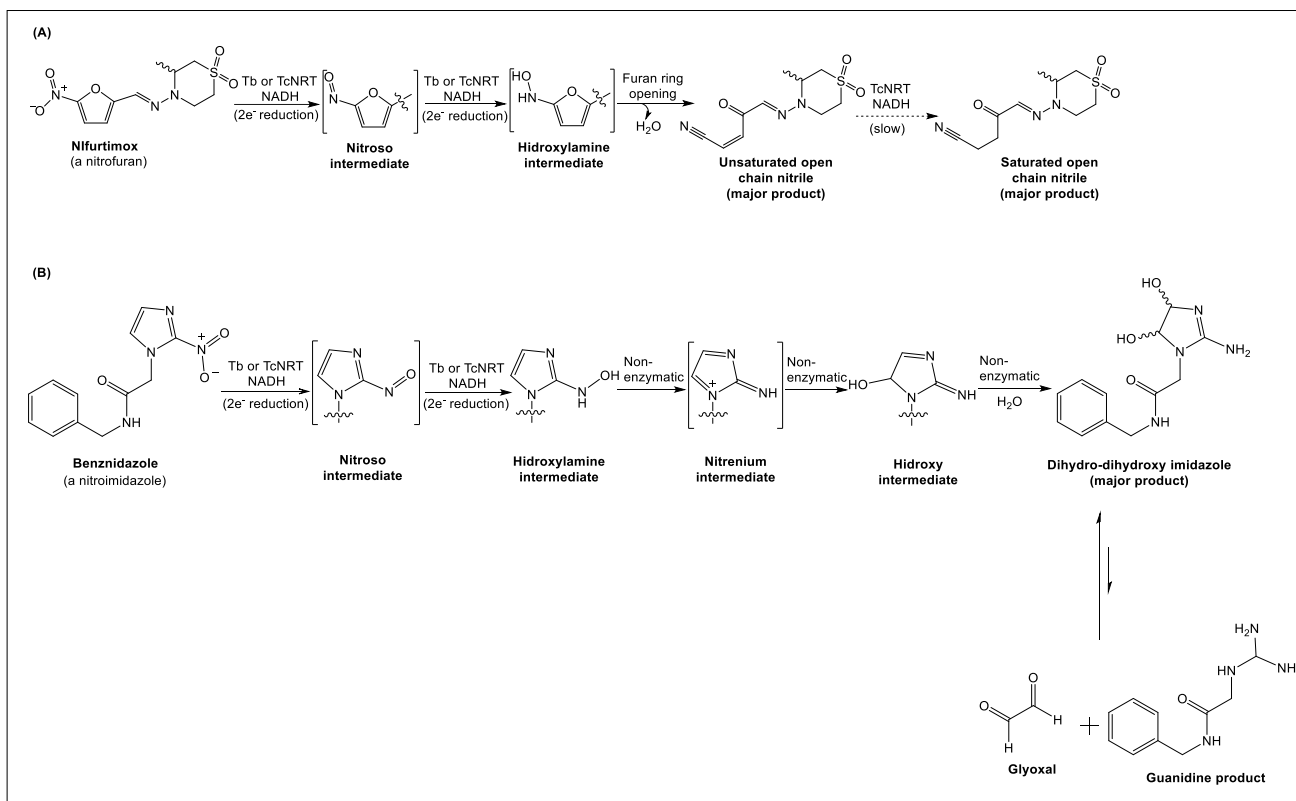


**Figure 4:** Schematic representation of the full reduction of the nitrocompounds benznidazole and nifurtimox by nitroreductases (Extracted from PATTERSON; WYLLIE, 2014).

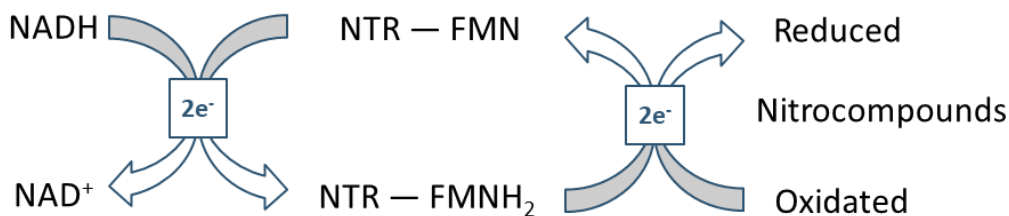


**Figure 5:** Representation of *T. cruzi* nitroreductase two substrate enzyme kinetics.

The exact physiological role of NTRs in bacteria or trypanosomatids is still unknown. In trypanosomes it is hypothesized that NTRs may function as ubiquinone reductases based on the mitochondrial location and preference for quinones. NTRs are also similar to FMN-dependent NADH dehydrogenases that reduces ubiquinone to ubiquinol using NADH as electron donor. This mechanism is essential in most organisms to maintain the NADH/NAD<sup>+</sup> balance in mitochondrion and the redox balance in the cell. In trypanosomes, several NADH reductases are reported but mitochondrial energetics of these parasites is not fully discovered and considerably varies according to the parasite form (HALL; MEREDITH; WILKINSON, 2012; WILKINSON et al., 2008a).

Regarding its therapeutic role, nitroreductases are involved in the activation of metronidazole, a 5-nitroimidazole, in bacteria (NILLIUS; MÜLLER; MÜLLER, 2011; WANG et al., 2016). The enzyme is also related to metronidazole resistant strains of *Helicobacter pilory* (MARTÍNEZ-JÚLVEZ et al., 2012) and the protozoan *Giardia lamblia* (MÜLLER; HEMPHILL; MÜLLER, 2018). In addition, it is described the role of a type I nitroreductase in the inactivation of chloramphenicol conferring resistance of *Haemophilus influenza* (CROFTS et al., 2019). Nitroreductases are also studied as candidates for a directed enzyme prodrug therapy for cancer treatment (PROSSER et al., 2013).

They are often homodimers with subunits of 20 to 30 kDa, globular, with a conserved domain for FMN/FAD binding at the dimer interface using NAD(P)H as an electron donor. Nitroreductases possess a characteristic  $\alpha+\beta$ -fold with a hydrophobic core of  $\beta$ -sheets surrounded by  $\alpha$ -helices (Figure 6). The helix  $\alpha_6$  is the responsible for the most of the dimer interactions along with the C-terminal portion that protrudes around the opposing monomer. The region comprising the  $\alpha_4$  and 5 is flexible, important to accommodate the different substrates described. The low identity between NTRs of trypanosomatids and bacteria can also explain the selectivity to different nitrocompounds (ROLDÁN et al., 2008).

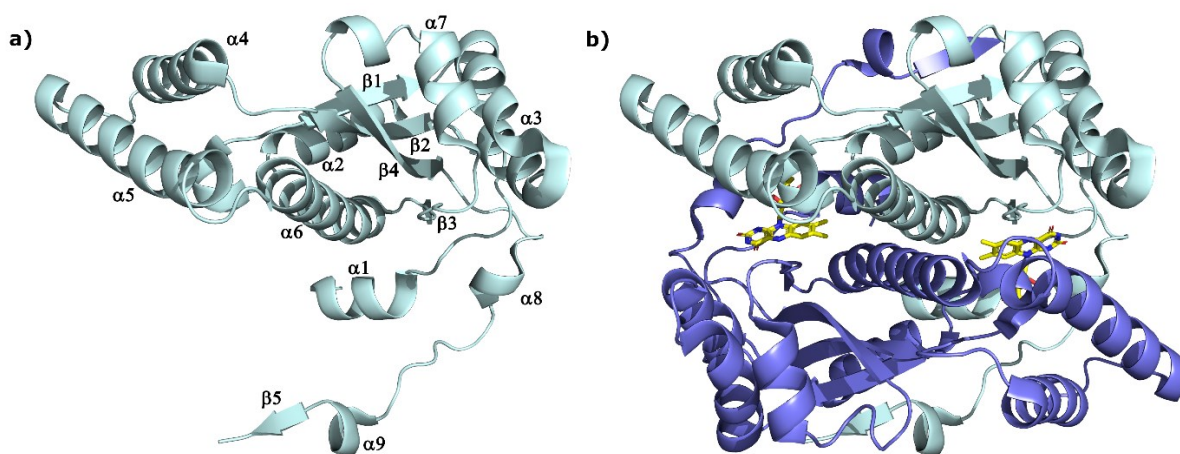


**Figure 6:** Cartoon representation of *E. coli* nitroreductase (PDB code: 1DS7) monomer (a) and dimer (b).

A type I NTR is absent in the human host which makes it an interesting target for new trypanocidal drugs. The side effects observed for the available drugs are a result of non-specific reduction by human enzymes (such as alcohol dehydrogenase 2 and P450 oxidoreductase) and metabolization by the intestinal microbial communities, which is

determinant for toxic metabolism of pollutant chemicals (HUNTER et al., 2015; PATTERSON; WYLLIE, 2014; ROLDÁN et al., 2008; ZHOU et al., 2012).

Considering the high number of infected people, the toxicity and lack of efficacy of available drugs, other therapeutic options must be searched. One possible strategy is to identify and characterize potential macromolecular targets for the development of new therapies. This work focuses on the characterization of TcNTR. The results of our studies will not only contribute to map the mechanism of activation of the available pro-drugs but also contribute to understand the role of NTR in *Trypanosoma cruzi*. Hence, a better evaluation of NTR structure is fundamental to the development more specific and effective drugs.

## 5. Final remarks and future perspectives

Considering the lack of effective treatments for Chagas disease, which still affects millions of people worldwide, the study of the enzyme nitroreductase is essential for the understanding not only of the mechanism of action of the two drugs available, but also for the NTR role in the parasite metabolism and how NTR can be better exploited for drug design.

In this study two gene constructs, TcNTR72 (residues 72 to 312) and TcNTR78 (residues 78 to 312), were evaluated. The construct TcNTR72 showed itself more stable probably due to a proper folding of structural elements at the N-terminal stretch. The expression protocol was successfully optimized leading to higher yields of purified protein. Optimization of the purification protocol led to higher thermal stability on both constructs.

The presence of detergent during purification is required to keep structural integrity, thermal stability, and activity of TcNTR. This result led us to investigate a possible interaction with membranes. For the first time, TcNTR was shown to interact with model membranes, in particular the ones containing cardiolipin, a lipid specific of mitochondrion, the cellular location for tripanossomatids NTRs.

Molecular modelling suggests an  $\alpha+\beta$  folding, characteristic of bacterial NTRs, despite the low sequential identity. The main difference is the fragment comprising residues 199 to 222 that is not present in the bacterial homologs. This region is hypothesized to be responsible for protein-membrane interaction.

Further studies, *in vitro* and *in silico*, for a better characterization of the TcNTR interaction with membranes will be performed. The complete structural characterization of TcNTR by single crystal X-ray diffraction was not achieved in this work and is important for a complete understanding of protein function and mechanism of selective activation of benznidazole and nifurtimox.

## Bibliography

ANDRADE, M. A. R. et al. Pendant-drop method coupled to ultraviolet-visible spectroscopy: A useful tool to investigate interfacial phenomena. **Colloids and Surfaces A: Physicochemical and Engineering Aspects**, v. 5, p. 305–311, 2016.

ARAÚJO, A. et al. Paleoparasitology of Chagas disease--a review. **Memorias do Instituto Oswaldo Cruz**, v. 104 Suppl, n. March, p. 9–16, 2009.

BERGER, M. JAMES; GAMBIN, J. STEVEN; HARRISON, C. STEPHEN; WANG, C. J. Structure and mechanism of DNA polymerases. **Nature**, v. 379, n. January, p. 225–232, 1996.

BERRY, J. D. et al. Measurement of surface and interfacial tension using pendant drop tensiometry. **Journal of Colloid and Interface Science**, v. 454, p. 226–237, 2015.

BOIVIN, S.; KOZAK, S.; MEIJERS, R. Optimization of protein purification and characterization using Thermofluor screens. **Protein Expression and Purification**, v. 91, n. 2, p. 192–206, 2013.

BOT, C. et al. Evaluating 5-nitrofurans as trypanocidal agents. **Antimicrobial Agents and Chemotherapy**, v. 57, n. 4, p. 1638–1647, 2013.

BRASIL; SAÚDE, M. DA. Doença de Chagas Aguda e distribuição espacial dos triatomíneos de importância epidemiológica, Brasil 2012 a 2016. **Boletim Epidemiológico**, v. 50, n. 2, p. 10, 2019.

CAMPOS, M. C. O. et al. Benznidazole-resistance in *Trypanosoma cruzi*: Evidence that distinct mechanisms can act in concert. **Molecular and Biochemical Parasitology**, v. 193, n. 1, p. 17–19, 2014.

CHENIOUR, M. et al. Evidence of proteolipid domain formation in an inner mitochondrial membrane mimicking model. **Biochimica et Biophysica Acta - General Subjects**, v. 1861, n. 5, p. 969–976, 2017.

CONNERS, E. E. et al. A global systematic review of Chagas disease prevalence among migrants. **Acta Tropica**, v. 156, p. 68–78, 2016.

COURA, R. Síntese histórica e evolução dos conhecimentos sobre a doença de chagas. **Clínica e terapêutica da doença de Chagas: uma abordagem prática para o clínico geral [online]**, 1997.

CROFTS, T. S. et al. Discovery and Characterization of a Nitroreductase Capable of

Conferring Bacterial Resistance to Chloramphenicol. **Cell chemical biology**, p. 1–12, 2019.

DE OLIVEIRA, I. M.; HENRIQUES, J. A. P.; BONATTO, D. In silico identification of a new group of specific bacterial and fungal nitroreductases-like proteins. **Biochemical and Biophysical Research Communications**, v. 355, n. 4, p. 919–925, 2007.

DEMETZOS, C. Differential Scanning Calorimetry (DSC): A tool to study the thermal behavior of lipid bilayers and liposomal stability. **Journal of Liposome Research**, v. 18, n. 3, p. 159–173, 2008.

DRAZENOVIC, J. et al. Effect of lamellarity and size on calorimetric phase transitions in single component phosphatidylcholine vesicles. **Biochimica et Biophysica Acta - Biomembranes**, v. 1848, n. 2, p. 532–543, 2015.

DROZDETSKIY, A. et al. JPred4: A protein secondary structure prediction server. **Nucleic Acids Research**, v. 43, n. W1, p. W389–W394, 2015.

DUROWOJU, I. B. et al. Differential Scanning Calorimetry &#8212; A Method for Assessing the Thermal Stability and Conformation of Protein Antigen. **Journal of Visualized Experiments**, n. 121, p. 1–8, 2017.

ERICSSON, U. B. et al. Thermofluor-based high-throughput stability optimization of proteins for structural studies. **Analytical Biochemistry**, v. 357, n. 2, p. 289–298, 2006.

GARCIA-GUERRERO, M. C. et al. Crystal structure and mechanism of human carboxypeptidase O: Insights into its specific activity for acidic residues. **Proceedings of the National Academy of Sciences**, v. 115, n. 17, p. E3932–E3939, 2018.

GARCÍA-HUERTAS, P. et al. Prostaglandin F<sub>2</sub> $\alpha$  synthase in trypanosoma cruzi plays critical roles in oxidative stress and susceptibility to benznidazole. **Royal Society Open Science**, v. 4, n. 9, p. 170773, 2017.

GONÇALVES, C. S. et al. Revisiting the Trypanosoma cruzi metacyclogenesis: Morphological and ultrastructural analyses during cell differentiation. **Parasites and Vectors**, v. 11, n. 1, p. 1–14, 2018.

GUHL, F.; AUDERHEIDE, A.; RAMÍREZ, J. D. From ancient to contemporary molecular eco-epidemiology of Chagas disease in the Americas. **International Journal for Parasitology**, v. 44, n. 9, p. 605–612, 2014.

HALL, B. S. et al. Exploiting the drug-activating properties of a novel trypanosomal nitroreductase. **Antimicrobial Agents and Chemotherapy**, v. 54, n. 3, p. 1193–1199, 2010.

HALL, B. S.; BOT, C.; WILKINSON, S. R. Nifurtimox activation by trypanosomal type I nitroreductases generates cytotoxic nitrile metabolites. **Journal of Biological Chemistry**, v. 286, n. 15, p. 13088–13095, 2011a.

HALL, B. S.; BOT, C.; WILKINSON, S. R. Nifurtimox activation by trypanosomal type I nitroreductases generates cytotoxic nitrile metabolites. **Journal of Biological Chemistry**, v. 286, n. 15, p. 13088–13095, 2011b.

HALL, B. S.; MEREDITH, E. L.; WILKINSON, S. R. Targeting the Substrate Preference of a Type I Nitroreductase To Develop Antitrypanosomal Quinone-Based Prodrugs. **Antimicrobial Agents and Chemotherapy**, v. 56, n. 11, p. 5821–5830, 2012.

HALL, B. S.; WILKINSON, S. R. Activation of benznidazole by trypanosomal type I nitroreductases results in glyoxal formation. **Antimicrobial Agents and Chemotherapy**, v. 56, n. 1, p. 115–123, 2012.

HAWE, A. et al. Taylor dispersion analysis compared to dynamic light scattering for the size analysis of therapeutic peptides and proteins and their aggregates. **Pharmaceutical Research**, v. 28, n. 9, p. 2302–2310, 2011.

HECHT, H. J. et al. Crystal structure of NADH oxidase from *Thermus thermophilus*. **Nature**, v. 2, n. 12, p. 1109, 1995.

HUNTER, F. W. et al. Identification of P450 oxidoreductase as a major determinant of sensitivity to hypoxia-activated prodrugs. **Cancer Research**, v. 75, n. 19, p. 4211–4223, 2015.

ISAYEV, O. et al. In silico structure-function analysis of *E. cloacae* nitroreductase. **Proteins: Structure, Function and Bioinformatics**, v. 80, n. 12, p. 2728–2741, 2012.

JOHNSON, C. M. Differential scanning calorimetry as a tool for protein folding and stability. **Archives of Biochemistry and Biophysics**, v. 531, n. 1–2, p. 100–109, 2013.

KASZUBA, M. et al. Measuring sub nanometre sizes using dynamic light scattering. **Journal of Nanoparticle Research**, v. 10, n. 5, p. 823–829, 2008.

KROPF, S. P. Doença de Chagas, doença do Brasil: ciência, saúde e nação (1909-1962). p. 600, 2006.

LEE, B. Y. et al. Global economic burden of Chagas disease: a computational simulation model. v. 13, n. 4, p. 342–348, 2013.

MARBLESTONE, J. G. Comparison of SUMO fusion technology with traditional gene fusion systems: Enhanced expression and solubility with SUMO. **Protein Science**, v. 15, n. 1, p. 182–189, 2006.

MARIN-NETO, J. A. et al. The BENEFIT trial: testing the hypothesis that trypanocidal therapy is beneficial. **Mem Inst Oswaldo Cruz, Rio de Janeiro**, v. 104, n. May, p. 319–324, 2009.

MARTIN, D. L. et al. *Trypanosoma cruzi* survival following cold storage: Possible implications for tissue banking. **PLoS ONE**, v. 9, n. 4, 2014.

MARTÍNEZ-JÚLVEZ, M. et al. Structure of RdxA: an oxygen insensitive nitroreductase essential for metronidazole activation in *Helicobacter pylori*. **FEBS Journal**, v. 279, n. 23, p. 4306–4317, 2012.

MCCUSKER, E. C. et al. Structure of a bacterial voltage-gated sodium channel pore reveals mechanisms of opening and closing. **Nature Communications**, v. 3, p. 1–8, 2012.

MEJÍA-JARAMILLO, A. M. et al. Gene expression study using real-time PCR identifies an NTR gene as a major marker of resistance to benznidazole in *Trypanosoma cruzi*. **Parasites and Vectors**, v. 4, n. 1, p. 169, 2011.

MEJIA, A. M. et al. Benznidazole-resistance in *trypanosoma cruzi* is a readily acquired trait that can arise independently in a single population. **Journal of Infectious Diseases**, v. 206, n. 2, p. 220–228, 2012.

MERKLEY, E. D.; PARSON, W. W.; DAGGETT, V. Temperature dependence of the flexibility of thermophilic and mesophilic flavoenzymes of the nitroreductase fold. **Protein Engineering, Design and Selection**, v. 23, n. 5, p. 327–336, 2010.

MÜLLER, J.; HEMPHILL, A.; MÜLLER, N. Physiological aspects of nitro drug resistance in *Giardia lamblia*. **International Journal for Parasitology: Drugs and Drug Resistance**, v. 8, n. 2, p. 271–277, 2018.

MURAKAMI, M. T. et al. Structural studies of the *Trypanosoma cruzi* Old Yellow Enzyme: Insights into enzyme dynamics and specificity. **Biophysical Chemistry**, v. 184, p. 44–53, 2013.

NILLIUS, D.; MÜLLER, J.; MÜLLER, N. Nitroreductase (GINR1) increases susceptibility of *Giardia lamblia* and *Escherichia coli* to nitro drugs. **Journal of Antimicrobial Chemotherapy**, v. 66, n. 5, p. 1029–1035, 2011.

PÁDUA, R. A. P. et al. ThermoFMN - A thermofluor assay developed for ligand-screening as an alternative strategy for drug discovery. **Journal of the Brazilian Chemical Society**, v. 25, n. 10, p. 1864–1871, 2014.

PANTOLIANO, M. W. et al. Pantoliano Thermofluor.pdf. **Journal of Biomolecular Screening**, v. 6, n. 6, p. 429–440, 2001.

PARADIES, G. et al. Functional role of cardiolipin in mitochondrial bioenergetics. **Biochimica et Biophysica Acta - Bioenergetics**, v. 1837, n. 4, p. 408–417, 2014.

PARKINSON, G. N.; SKELLY, J. V.; NEIDLE, S. Crystal Structure of FMN-Dependent Nitroreductase from *Escherichia coli* B: A. **J. Med. Chem.**, n. 43, p. 3624–3631, 2000.

PATTERSON, S.; WYLLIE, S. Nitro drugs for the treatment of trypanosomatid diseases: Past, present, and future prospects. **Trends in Parasitology**, v. 30, n. 6, p. 289–298, 2014.

PÉREZ-MOLINA, J. A. et al. Old and new challenges in Chagas disease. **The Lancet Infectious Diseases**, v. 15, n. 11, p. 1347–1356, 2015.

PÉREZ-MOLINA, J. A.; MOLINA, I. Chagas disease. **The Lancet**, v. 391, p. 82–94, 2017.

PEREZ, C. J.; LYMBERG, A. J.; THOMPSON, R. C. A. Reactivation of Chagas Disease: Implications for Global Health. **Trends in Parasitology**, v. 31, n. 11, p. 595–603, 2015.

PROSSER, G. A. et al. Creation and screening of a multi-family bacterial oxidoreductase library to discover novel nitroreductases that efficiently activate the bioreductive prodrugs CB1954 and PR-104A. **Biochemical Pharmacology**, v. 85, n. 8, p. 1091–1103,

2013.

ROBERTSON, L. J. et al. Trypanosoma cruzi: Time for International Recognition as a Foodborne Parasite. **PLoS Neglected Tropical Diseases**, v. 10, n. 6, p. 3–8, 2016.

ROLDÁN, M. D. et al. Reduction of polynitroaromatic compounds: The bacterial nitroreductases. **FEMS Microbiology Reviews**, v. 32, n. 3, p. 474–500, 2008.

SAAD, S. M. I.; POLICOVA, Z.; NEUMANN, A. W. Design and accuracy of pendant drop methods for surface tension measurement. **Colloids and Surfaces A: Physicochemical and Engineering Aspects**, v. 384, n. 1–3, p. 442–452, 2011.

SANTOS, S. P. et al. Thermofluor-based optimization strategy for the stabilization and crystallization of Campylobacter jejuni desulforubrythrin. **Protein Expression and Purification**, v. 81, n. 2, p. 193–200, 2012.

SCHLAME, M.; REN, M. The role of cardiolipin in the structural organization of mitochondrial membranes. **Biochimica et Biophysica Acta - Biomembranes**, v. 1788, n. 10, p. 2080–2083, 2009.

SONG, H. N. et al. Crystal structure of the fungal nitroreductase Frm2 from Saccharomyces cerevisiae. **Protein Science**, v. 24, n. 7, p. 1158–1163, 2015.

SPINK, C. H. Differential Scanning Calorimetry. **Methods in Cell Biology**, v. 84, n. 7, p. 115–141, 2008.

STANAWAY, J. D.; ROTH, G. The Burden of Chagas Disease Estimates and Challenges. **Global Heart**, v. 10, n. 3, p. 139–144, 2015.

STEVERDING, D. The history of Chagas disease. **Parasites and Vectors**, v. 7, n. 1, p. 1–8, 2014.

STUDIER, F. W. Protein production by auto-induction in high density shaking cultures. **Protein expression and purification**, v. 41, n. 1, p. 207–234, 2005.

TEIXEIRA, D. E. et al. Interactive Multimedia to Teach the Life Cycle of Trypanosoma cruzi, the Causative Agent of Chagas Disease. **PLoS Neglected Tropical Diseases**, v. 6, n. 8, p. e1749, 2012.

VOAK, A. A. et al. An essential type I nitroreductase from leishmania major can be used to activate leishmanicidal prodrugs. **Journal of Biological Chemistry**, v. 288, n. 40, p. 28466–28476, 2013.

WANG, B. et al. Crystal structures of two nitroreductases from hypervirulent Clostridium difficile and functionally related interactions with the antibiotic metronidazole. **Nitric Oxide - Biology and Chemistry**, v. 60, p. 32–39, 2016.

WATERHOUSE, A. et al. SWISS-MODEL: Homology modelling of protein structures and complexes. **Nucleic Acids Research**, v. 46, n. W1, p. W296–W303, 2018.

WEIDS, A. J. et al. Distinct stress conditions result in aggregation of proteins with similar properties. **Scientific Reports**, v. 6, 2016.

WEINBERG, R. B. et al. Interfacial exclusion pressure determines the ability of apolipoprotein A-IV truncation mutants to activate cholesterol ester transfer protein. **Journal of Biological Chemistry**, v. 277, n. 24, p. 21549–21553, 2002.

WILKINSON, S. R. et al. A mechanism for cross-resistance to nifurtimox and benznidazole in trypanosomes. **Proceedings of the National Academy of Sciences**, v. 105, n. 13, p. 5022–5027, 2008a.

WILKINSON, S. R. et al. A mechanism for cross-resistance to nifurtimox and benznidazole in trypanosomes. **Proceedings of the National Academy of Sciences**, v. 105, n. 13, p. 5022–5027, 2008b.

XU, D.; ZHANG, Y. Ab initio protein structure assembly using continuous structure fragments and optimized knowledge-based force field. **Proteins: Structure, Function and Bioinformatics**, v. 80, n. 7, p. 1715–1735, 2012.

XU, D.; ZHANG, Y. Toward optimal fragment generations for ab initio protein structure assembly. **Proteins: Structure, Function and Bioinformatics**, v. 81, n. 2, p. 229–239, 2013.

YANG, J. et al. The I-TASSER suite: Protein structure and function prediction. **Nature Methods**, v. 12, n. 1, p. 7–8, 2014.

ZHOU, L. et al. ALDH2 mediates 5-nitrofurantoin activity in multiple species. **Chemistry and Biology**, v. 19, n. 7, p. 883–892, 2012.